High Resolution Charge-based Electrokinetic Separation of Almost Identical Microparticles

Alaleh Vaghef-Koodehi,[†] Curran Dillis[†] and Blanca H. Lapizco-Encinas[†,*]

[†] Microscale Bioseparations Laboratory and Biomedical Engineering Department, Rochester Institute of Technology, 160 Lomb Memorial Drive, Rochester, New York, 14623, United States;

Blanca H. Lapizco-Encinas (PhD)
Email: bhlbme@rit.edu

Keywords:
Electrokinetics
Electrophoresis
Insulators
Microfluidics
Microparticles

ABSTRACT: Well-established techniques, e.g., chromatography and capillary electrophoresis, are available for separating nano-sized particles, such as proteins. However, similar techniques for separating micron-sized particles are still needed. Insulator-based electrokinetic (iEK) systems can achieve efficient microparticle separations by combining linear and nonlinear EK phenomena. Of particular interest are charge-based separations, which could be employed for separating similar microorganisms, such as bacterial cells of the same size, same genus, or same strain. Several groups have reported charge-based separations of microparticles where a zeta potential difference of at least 40 mV between the microparticles was required. The present work pushes the limit of the discriminatory capabilities of iEK systems by reporting the charged-based separation of two microparticles of the same size (5.1 μm), same shape, same substrate material, and with a small difference in particle zeta potentials of only 3.6 mV, which is less than 10% of the difference in previous studies. By building an accurate COMSOL *Multiphysics* model, which correctly accounts for dielectrophoresis and electrophoresis of the second kind, it was possible to identify the conditions to achieve this challenging separation. Furthermore, the COMSOL model allowed predicting particle retention times ($t_{R,p}$) which were compared with experimental values ($t_{R,e}$). The separations results had excellent reproducibility in terms of $t_{R,e}$ with variations of only 9% and 11% between repetitions. These findings demonstrate that by following a robust protocol that involves modeling and experimental work, it is possible to discriminate between highly similar particles, with much smaller differences in electrical charge than previously reported.

Traditional well-established techniques, e.g., chromatography and capillary electrophoresis, are available for analyzing nano-sized bioparticles, such as macromolecules. However, similar reliable techniques are not available for separating micron-sized particles, including intact microorganisms.[1] Microfluidic devices are robust platforms for the rapid analysis of a wide range of particles, from macromolecules to parasites.[1–3] An important microfluidics subfield is electrokinetics (EK), which refers to the manipulation of particles and fluid with electric fields. Electrokinetics allows combining several EK phenomena within the same system, providing ample options when designing separation processes for bioparticles, such as cells,[4] cell organelles,[5] and exosomes.[6] Electrokinetic phenomena are classified as linear and nonlinear based on their dependence on the electric field. Many successful EK-based systems combine linear and nonlinear EK phenomena within the same device.[7] By varying the magnitude of the applied electric potential, it is possible to shift from linear to nonlinear EK phenomena, making it straightforward to switch between EK regimes.

Insulator-based EK (iEK) systems employ insulating structures to distort the electric field distribution, creating regions of higher field intensity within a system; nonlinear EK phenomena are enhanced in these regions, making iEK devices ideal for combining EK regimes.[8] iEK systems have been used in many applications, from protein enrichment to the analysis of neural stem cells.[3,9] Thus, there is a growing interest in advancing the discriminatory capabilities of iEK systems to allow for separations of highly similar micron-sized particles, such as cells of the same size, same genus or same strain. Several groups have studied charge-based separations of microparticles, by exploiting differences in particle zeta potential (ζ_P) values from 40 to 63 mV.[10–15] Two recent reports from our group[10,11] demonstrated the charge-based separation of two types of 10 μm particles with a difference in ζ_P values of 40 mV employing low-frequency cyclical potentials and DC potentials. In 2009, the Verpoorte group[12] investigated the charge-based separation of 3 μm polystyrene particles with a difference in ζ_P values of 40 mV, by combining hydrodynamic and EK forces in a diverging-converging device. The Xuan group demonstrated in 2013[15] the charge-based separation of 3 μm fluorescent and nonfluorescent polystyrene microparticles with a difference in ζ_P values of 40 mV using a technique called reservoir-based dielectrophoresis (DEP) in a microchannel with a constricted region under AC potentials at 1 kHz. In 2011, the Xuan group[14] reported the charge-based separation of two types of 10 μm particles with a large difference in their linear EK mobility (ζ_P values were not reported), employing curvature induced DEP. Recently, in 2019, Calero *et al.*[13] reported the charge-based separation of two types of 3 μm with a difference in ζ_P values of 63 mV by combining deterministic lateral displacement (DLD) in an iEK device with a dense insulating post array under AC potentials at 100 Hz.

Very recent developments[16–19] illustrated the effects of the nonlinear phenomena of electrophoresis of the second kind ($EP^{(3)}$) on particle migration in iEK systems. This new knowledge allows, for the first time, to accurately model and predict particle migration and behavior in iEK systems.[8] Prior iEK studies required the use of empirical correction factors[7,20] added to the mathematical models to achieve agreement with experimental results. In those studies, DEP was considered strong enough to balance other EK forces in the systems and generate particle trapping.[21] Recent studies[16–19] revealed that particle trapping in iEK systems, stimulated with direct current (DC) potentials, is mainly the result of a balance between electroosmotic (EO) flow and electrophoresis (linear $EP^{(1)}$ and nonlinear $EP^{(3)}$). DEP is *still* a force present in DC-iEK systems, but it is not dominant, representing less than 6% of the magnitude of $EP^{(3)}$.[22] It is now believed that the main reason for requiring correction factors when modeling DC-iEK systems under high electric fields, was that DEP effects were inaccurately considered and $EP^{(3)}$ effects were neglected.[7,8]

This work reports the charged-based binary separation of almost identical polystyrene microparticles in an iEK device. The microparticles had the same size (5.1 μm), same shape, were made by the same manufacturer from the same substrate material, and only had a small difference in the particle zeta potential of 3.6 mV, which is less than 10% of the ζ_P difference required by previous similar studies, which ranged from 40 to 63 mV.[10–15] This study pushes the limit of the discriminatory capabilities of iEK systems. By employing computational modeling with COMSOL *Multiphysics*, which properly considers $EP^{(1)}$, $EP^{(3)}$, EO flow, and DEP, it was possible to accurately predict the electrical potentials required for the charged-based separation of almost identical microparticles. The COMSOL model also predicted particle retention times ($t_{R,p}$) which were compared with experimental particle retention times ($t_{R,e}$), where deviations of 32% and 2%, were obtained. The reproducibility between experimental repetitions showed deviations in $t_{R,e}$ of only 9 and 11%. This is the first report of modeling predictions of particle retention time in an iEK system. These results demonstrate that combining insulating posts with proper consideration of nonlinear EK effects, results in tunable separations, making it possible to discriminate between highly similar particles, with much smaller differences in electrical charge, than previous studies.

THEORY AND COMPUTATIONAL MODEL

In iEK systems under DC electric potentials, EO and $EP^{(1)}$ are the dominant linear EK mechanisms, while DEP and $EP^{(3)}$ are the main nonlinear phenomena. The expressions for the EO and $EP^{(1)}$ velocities are as follows:[17]

$$\mathbf{v}_{EO} = \mu_{EO}\mathbf{E} = -\frac{\varepsilon_m \zeta_W}{\eta}\mathbf{E} \quad (1)$$

$$\mathbf{v}_{EP}^{(1)} = \mu_{EP}^{(1)}\mathbf{E} = \frac{\varepsilon_m \zeta_P}{\eta}\mathbf{E} \quad (2)$$

where $\mathbf{v}$ is the velocity, μ is mobility, ε_m and η are the medium electric permittivity and viscosity, ζ is zeta potential of the particle or channel wall, and $\mathbf{E}$ is the electric field, respectively. The velocity expressions for the nonlinear EK phenomena of DEP and $EP^{(3)}$ are:

$$\mathbf{v}_{DEP} = \mu_{DEP}\nabla E^2 = \frac{r_p^2 \varepsilon_m}{3\eta}\mathrm{Re}[f_{CM}]\nabla E^2 \quad (3)$$

$$\mathbf{v}_{EP}^{(3)} = \mu_{EP}^{(3)}\mathbf{E^3} \quad (4)$$

where r_p is the particle diameter and $\mathrm{Re}(f_{CM})$ is the real part of the Clausius-Mossotti factor (f_{CM}), which accounts for the particle polarizability relative to that of the suspending medium. The f_{CM} for both particles was assumed as -0.5,[23] as the electrical conductivity of the microparticles is much lower than that of the medium, thus, all microparticles exhibited negative DEP behavior. A dependence with $\mathbf{E}^3$ is assumed for $EP^{(3)}$ under the current operating conditions.[16,19] The overall particle velocity in the iEK microchannel shown in **Figure 1a** is the result of

the four EK phenomena depicted in **Figure 1b** for negatively charged particles. Recent studies[16,18,19,22] demonstrated that the DEP velocity magnitude is much lower than that of the other three phenomena, thus, the overall velocity expression can be simplified by removing the DEP term:

$$\mathbf{v}_P = \mathbf{v}_{EO} + \mathbf{v}_{EP}^{(1)} + \mathbf{v}_{EP}^{(3)} \quad (5)$$

Cardenas-Benitez[16] recently proposed the parameter of EK equilibrium condition (E_{EEC}) to identify the electric field at which particle trapping is reached when $\mathbf{v}_P = 0$. The E_{EEC} parameter is needed for estimating $\mu_{EP}^{(3)}$ of particles. The particles employed in this study were characterized in terms of their EP mobilities ($\mu_{EP}^{(1)}$ and $\mu_{EP}^{(3)}$) and E_{EEC} (**Table 1**). Equation (6) illustrates the expression for E_{EEC} which is obtained by setting $\mathbf{v}_P = 0$ in Eqn. (5), and Eqn. (7) contains the expression for estimating $\mu_{EP}^{(3)}$ used in this study.

$$E_{EEC} = \sqrt{-\frac{\left(\mu_{EP}^{(1)} + \mu_{EO}\right)}{\mu_{EP}^{(3)}}} \quad (6)$$

$$\mu_{EP}^{(3)} = -\frac{\left(\mu_{EP}^{(1)} + \mu_{EO}\right)}{{E_{EEC}}^2} \quad (7)$$

The quality of the microparticle separations was assessed by employing the well-known parameters of resolution (Rs) and number of plates (N), illustrated in Eqns. (8)-(9), where W is the width of the peak at the base.

$$Rs = \frac{2\,(t_{R2,e} - t_{R1,e})}{W_1 + W_2} \quad (8)$$

$$N = \frac{16\ {t_{R,e}}^2}{W^2} \quad (9)$$

A computational model was built with COMSOL *Multiphysics*® 4.4 (COMSOL Inc. Burlington, MA, USA) to study the electric field distribution across the device shown in **Figure 1a.** The model solved the Laplace equation with appropriate boundary conditions illustrated in **Figure S1** and **Table S1** in the supporting information file.

The EK properties of the microparticles (**Table 1**) were experimentally determined as described in the experimental section. Particle data was then introduced to COMSOL to select the voltages that allowed particles to be effectively injected into the channel. A set of four voltages were selected for each one of the three steps in the EK injection process; these steps are loading, gating, and injection (**Table 2)**. The voltages employed in the last step of the injection process, which is when the separation takes place, were used for predicting the $t_{R,p}$ values (**Table 1)**, which were compared with the experimental $t_{R,e}$ values. Predicted $t_{R,p}$ values were calculated employing particle velocities over the cutline shown in **Figure S2**.

EXPERIMENTAL SECTION

Microdevices. Microdevices were made from polydimethylsiloxane (PDMS, Dow Corning, MI, USA) employing standard soft lithography methods as previously reported.[24] The microchannels were standard EK injection T-designs, with asymmetric insulating posts, a depth of 40 μm, and the dimensions shown in **Figure 1a**.

Suspending medium and microparticles. The suspending medium was a 0.2 mM solution of K_2HPO_4, with 0.05% (v/v) of Tween 20 to prevent microparticle clumping. The medium had a conductivity of 40.7 μS/cm and a pH of 7.3 which was adjusted by using a 0.1 N KOH solution; this medium produced a ζ_W = -60.1 mV and μ_{EO} = 4.68×10$^-$

^{8} $m^2V^{-1}s^{-1}$ in the PDMS devices, as measured with current monitoring.[25] Two types of negatively charged 5.1 µm polystyrene microparticles (Magsphere Pasadena, CA, USA) were used (**Table 1)** at a concentration of 1.2x10^{8} particles/mL. The ζ_P and E_{EEC} of the particles was characterized with particle image velocimetry (PIV) employing a series of low and high voltages in a channel without posts[16,17] and the $\mu_{EP}^{(3)}$ was estimated with Eqn. (7).

Equipment and software. Videos of experiments were recorded with a Leica DMi8 (Wetzlar, Germany) inverted microscope. A high voltage power supply (Model HVS6000D, LabSmith, Livermore, CA) was employed to apply DC electric potentials to the device by employing four distinct platinum wire electrodes labeled A-D (**Fig. 1a**).

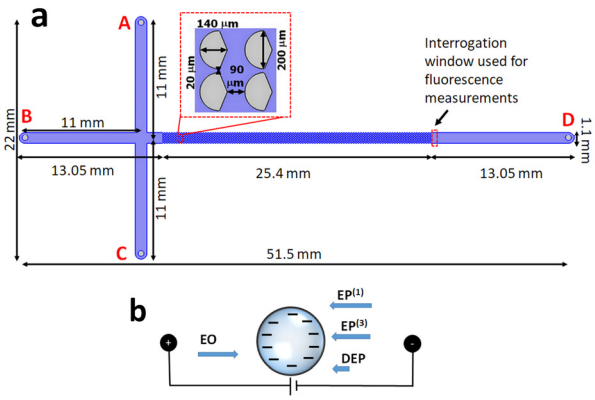

Figure 1. (a) Microchannel representation depicting insulating posts and channel dimensions, and the location of the fluorescence interrogation window. The labels A-D refer to the four electrodes (Table 2). **(b).** Illustration as arrows of the four EK phenomena acting on the negatively charged microparticles.

Table 1. Characteristics of the microparticles used in this study, including the separation results in terms of $t_{R,p}$ and $t_{R,e}$.

Particle ID	Diameter (µm)	ζ_P (mV)	$\mu_{EP}^{(1)}$ x 10^{-8} ($m^2V^{-1}s^{-1}$)	E_{EEC} (V/cm)	$\mu_{EP}^{(3)}$ x 10^{-19} ($m^4V^{-3}s^{-1}$)	COMSOL predicted ($t_{R,p}$) (s)	Experimental ($t_{R,e}$) (s)	DEV. (%)
Particle 1 (red)	5.1	-27.2 ± 1.5	-2.1 ± 0.1	1,780.9 ± 3.3	-11.2 ± 0.1	148.9	113	32
Particle 2 (green)	5.1	-30.8 ± 0.4	-2.4 ± 0.1	2,696.4 ± 46.2	-5.1 ± 0.2	166.8	170	2

Table 2. Voltages employed for EK sample injection and iEK charge-based microparticle separation.

Step	Run time (s)	Applied Voltage (V)			
		Reservoir A	Reservoir B	Reservoir C	Reservoir D
Loading	7.5	1500	100	0	1000
Gating	1	2000	2000	2000	0
Injection	350	200	500	200	0

Experimental procedure. Microchannels were filled with the suspending medium 12-16 hours before experimentation to ensure a stable EO flow. Large liquid reservoirs (~4 mL) were employed to decrease pressure-driven flow. After introducing 10 µL of the microparticle suspensions into reservoir A (**Fig. 1a**), platinum wire electrodes were placed into the four reservoirs. For EK sample injection, three distinct sets of voltages were applied (**Table 2**) to follow the steps: loading, gating, and injection.[2,26] With an EK injection process, there is uneven particle distribution at the intersection of the T-device, which allows the red particles, that have the higher μ_{EK}, to migrate further.[26] The run time refers to the duration of each voltage step, the duration of the injection step was

determined by the time required for the particles to elute from the post array.

RESULTS AND DISCUSSION

After microparticles properties were assessed with a series of PIV experiments, COMSOL *Multiphysics* was employed for predicting $t_{R,p}$ values in the insulating-post array, and these values were compared with $t_{R,e}$ (**Table 1**). The voltages identified with COMSOL for the EK sample injection and microparticle separation (**Table 2**), were used for experimentation. This was the protocol employed in this work: i) characterization of microparticles, ii) COMSOL simulations to identify proper voltages, and iii) fine-tuning of the EK injection process and experimental separation of the microparticles. It was identified that the duration of the EK injection steps was critical, in particular the gating step required significant fine-tuning to ensure the success of the separation. The electropherogram of one of the iEK separations (repetition 1, **Table S2**) of these two types of highly similar particles is reported in **Figure 2a**. The peaks in **Figure 2a** were built by employing the fluorescence signal from the particles, as they eluted the insulating post array (**Video S1**). As observed, the two peaks are well-defined, with the red particle (particle 1) eluting first ($t_{R1,e}$ = 113 s) and the green particle (particle 2) eluting second ($t_{R2,e}$= 170 s). The experiments were performed four times (**Table S2**) and excellent reproducibility was obtained, the deviations in $t_{R,e}$ were only 11% and 9% for the red and green particle, respectively. Also, the $t_{R,e}$ values are in a fair agreement with the COMSOL $t_{R1,p}$ values (**Table 1)**, with deviations of 32% and 2% for the red and green particles, respectively. This level of accuracy between simulations and experiments is a significant step forward, as previous studies required correction factors of two orders of magnitude.[11] This study is the first report of particle retention times in an iEK device, where experimental and modeling results are compared and in fair agreement without correction factors.[20]

The red particles eluted from the post array more rapidly than predicted with COMSOL (**Table 1**, 149 s vs. 113 s). A potential cause for this higher deviation between modeling end experimental results could be "injection bias," which is a normally occurring phenomenon in EK injections; where higher mobility particles are prompted more than lower mobility particles.[26] In this case, injection bias causes the red particles to be "ahead" of the green particles, at the time the last EK injection step started, giving the red particles an advanced location, thus, reducing its experimentally assessed retention time. Care was taken in fine-tuning the gating step to decrease injection bias, but this effect cannot be completely eliminated. Another potential cause for the shorter than expected $t_{R1,e}$ value could be particle-particle interactions. When the red particles elute, they do so in the presence of a large number of green particles. The particles themselves act as insulators[27] that also distort the electric field distribution, affecting particle migration velocity. The COMSOL model considers the contributions of four EK phenomena for estimating $t_{R,p}$, but it does not consider particle-particle interactions and the distortion to the electric field caused by the particles themselves. However, in the actual experimental trial, these effects not considered by the COMSOL model, can significantly affect particle migration and $t_{R,e}$ values.

Figure 2b shows the two types of particles forming "zones" as they migrate across the insulating post array, with the red particles getting ahead of the green particles, illustrating the higher overall velocity of the red particles. This experimental observation is in agreement with the particle properties (**Table 1**), theory, and the model predictions, which are listed in detail in **Table S3** and plotted in **Figure 2c**. Since particle 1 (red) has a lower magnitude negative ζ_P , *i.e.*, a lower magnitude $EP^{(1)}$ force towards the inlet is exerted on the red particle (**Fig. 1b**), allowing the red particle to have a higher overall velocity towards the outlet. The small difference in ζ_P of 3.6 mV between the

particles allows the red particle to migrate forward faster than the green particle, as illustrated in **Figure 2a-2b**.

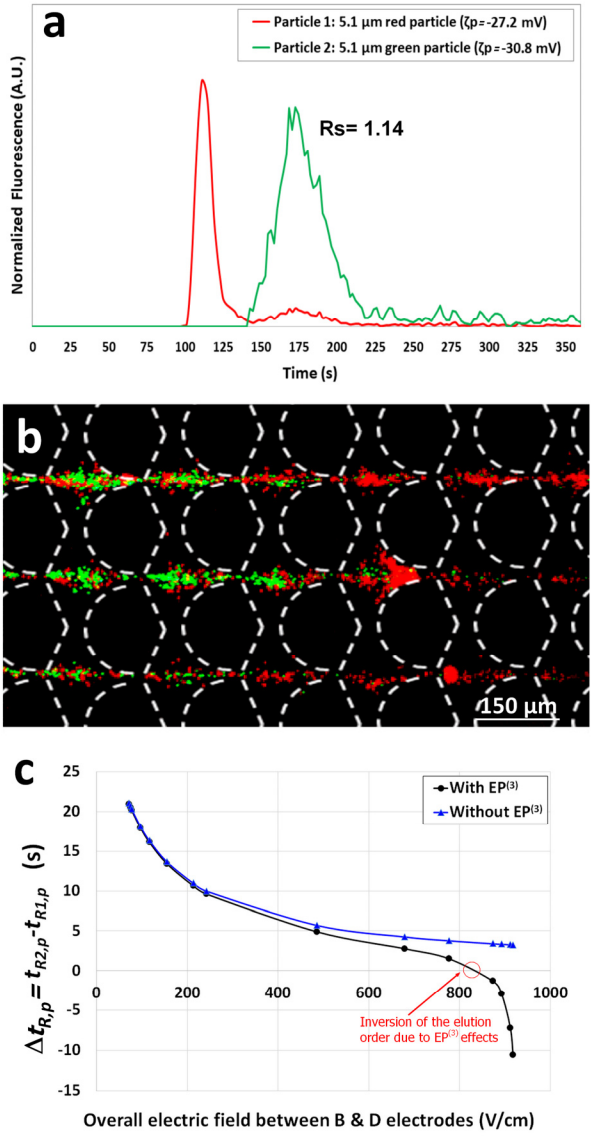

Figure 2. Separation of highly similar microparticles by exploiting small charge differences. **(a)** Electropherogram of the microparticle separation of built employing fluorescence signal. **(b)** Image of the microparticles as they begin to separate in "zones" within the post array, illustrating that the red particles are getting ahead of the green particles. A video of this separation is included as supporting information **Video_S1.mp4**. **(c)** Computational model predictions of particle retention times illustrated as a plot of $\Delta t_{R,p}$ as a function of the electric field, where a change in the elution order is observed at electric fields >875 V/cm.

However, the magnitude of the negative $\mu_{EP}^{(3)}$ of the red particle is higher than that of the green particle, which negatively affects this separation. Considering this, the applied voltages were carefully chosen with COMSOL (**Table S3** and **Fig. 3**) to ensure that the separation takes place under the streaming iEK regime, where the effects of the linear $EP^{(1)}$ dominate the system and enable a successful charge-based separation. The effects of $EP^{(3)}$ were carefully controlled by keeping the applied voltages low (ΔV = 500 V between electrodes B & D, resulting in overall **E** = 97.1 V/cm), so the separation could occur with the red particle eluting first. **Figure S4** in the supporting information illustrates the relative magnitudes of all EK phenomena exerted on the particles, confirming that at the

selected voltages, $EP^{(3)}$ effects were kept low. A rather long iEK device had to be used to make this separation possible, as the only distinction between these two types of particles was a small difference in ζ_P values of 3.6 mV. A device with asymmetric insulating posts was used, since prior studies[11,28] illustrated the discriminatory capabilities of these devices. The post asymmetry creates an asymmetric distribution of the electric field, which enhances small differences in particle electromigration velocity as illustrated by the particle zones in **Figure 2b**.

The electropherogram in **Figure 2a** has a resolution of *Rs* =1.14 (Eqn. 8), which are encouraging results as these particles are almost identical: same size, same shape, same substrate material, and same manufacturer. The number of plates illustrates the efficiency of the separation, where the results are N_1 = 1,419 and N_2 = 514 (Eqn. 9) for the red and green particles, respectively; N_1 is higher than N_2 since the red particle peak is narrower. Considering that the length of the post array is 2.54 mm, this results in separation efficiencies, expressed as *N/meter*, of 55,857 and 20,227 plates/meter for the red and green particles, respectively, which are comparable to those obtained with protein separations in capillary electrophoresis systems.[29] An important aspect is that the separation reported here is for 5 μm particles, not nano-sized protein particles; therefore, achieving results similar to those obtained with proteins is encouraging. To further study the effect of $EP^{(3)}$, **Figure 2c** shows a summary of the computational model results, which are also listed in detail in **Table S3** and **Figure S3**. As expected, the elution order of the particles, reported as $\Delta t_R = t_{R2,p} - t_{R1,p}$, is reversed at electric fields > 875 V/cm; this is caused by the higher magnitude of the negative $\mu_{EP}^{(3)}$ of the red particle, at higher voltages, the red particles are "pulled" stronger towards the inlet than the green particles. The simulations in **Figure 2c** were stopped when the particle velocity became zero (trapping) or negative (migration towards the inlet), since under these conditions the separation can no longer occur under the iEK streaming regime.

This computational model, which properly considers the effects of $EP^{(3)}$ and DEP, can predict particle migration behavior accurately. No correction factors are used to increase DEP effects, as previously done,[20] and for the first time $EP^{(3)}$ effects are considered. This report demonstrates that with carefully selected conditions and with the aid of accurate mathematical models, it is possible to design separation processes for micron-sized particles that are analogous to the well-established methods available for nano-sized particles, such as proteins. This study is the first charge-based separation of almost identical microparticles; previous similar studies have not achieved this high discriminatory capacity.

CONCLUSIONS

By following a robust protocol that combines accurate computational models, that consider linear and nonlinear EK phenomena, with careful experimentation, it is possible to carry out highly discriminatory microparticle separations. By properly accounting for $EP^{(3)}$ and DEP effects, the resulting COMSOL model allowed identifying appropriate voltages for the charged-based separation, the model also predicted microparticle retention times that were in good agreement with experimentally measured retentions times. The separation of two almost identical types of 5.1 μm particles was successfully achieved with excellent reproducibility by exploiting a charge difference of only 3.6 mV, which is less than 10% of the charge difference required by prior similar studies.[10–15] These results demonstrate that the combination of insulating posts with proper consideration of nonlinear EK effects results in highly tunable separations, where it is possible to exploit much smaller charge differences to successfully separate highly similar micron-sized particles.

ASSOCIATED CONTENT

Supporting Information
The Supporting Information is available free of charge on the ACS Publications website. It contains a file with the model information (**Figs. S1-S2** and **Table S1**), experiment reproducibility (**Table S2**), predicted particle retention time (**Table S3** and **Figure S3**), and particle velocities components over one constriction (**Figure S4**). **Video_S1.mp4** shows the microparticle elution and the plotting of the fluorescence signal from **Figure 2a**.

AUTHOR INFORMATION
Corresponding Author
Email: bhlbme@rit.edu

ORCID
Blanca H. Lapizco-Encinas: 0000-0001-6283-8210

Author Contributions
AVK: Experimentation, Data Analysis, Writing Original Draft – Review & Editing. **CD**: Experimentation, Data Analysis, Writing Original Draft – Review & Editing. **BHLE**: Conceptualization, Methodology, Data Analysis, Project administration, Supervision, Writing Original Draft – Review & Editing.

Notes:
The authors declare no competing financial interest.

ACKNOWLEDGMENTS

The authors acknowledge the financial support provided by the National Science Foundation (Awards CBET-1705895 and CBET-2127592).

REFERENCES

(1) Vaghef-Koodehi, A.; Lapizco-Encinas, B. H. Microscale Electrokinetic-Based Analysis of Intact Cells and Viruses. *Electrophoresis* **2022**, *43* (1–2), 263–287. https://doi.org/10.1002/elps.202100254.
(2) Miller, A.; Hill, N.; Hakim, K.; Lapizco-Encinas, B. H. Fine-Tuning Electrokinetic Injections Considering Nonlinear Electrokinetic Effects in Insulator-Based Devices. *Micromachines 2021, Vol. 12, Page 628* **2021**, *12* (6), 628. https://doi.org/10.3390/mi12060628.
(3) Lapizco-Encinas, B. H. Microscale Electrokinetic Assessments of Proteins Employing Insulating Structures. *Curr. Opin. Chem. Eng.* **2020**, *29*, 9–16. https://doi.org/10.1016/J.COCHE.2020.02.007.
(4) Liu, Y.; Hayes, M. A. Differential Biophysical Behaviors of Closely Related Strains of Salmonella. *Front. Microbiol.* **2020**, *11*, 302. https://doi.org/10.3389/FMICB.2020.00302/BIBTEX.
(5) Kim, D.; Luo, J.; Arriaga, E. A.; Ros, A. Deterministic Ratchet for Sub-Micrometer (Bio)Particle Separation. *Anal. Chem.* **2018**, *90* (7), 4370–4379. https://doi.org/10.1021/acs.analchem.7b03774.
(6) Shi, L.; Esfandiari, L. An Electrokinetically-Driven Microchip for Rapid Entrapment and Detection of Nanovesicles. *Micromachines* **2020**, *12* (1), 11. https://doi.org/10.3390/mi12010011.
(7) Perez-Gonzalez, V. H. Particle Trapping in Electrically Driven Insulator-Based Microfluidics: Dielectrophoresis and Induced-Charge Electrokinetics. *Electrophoresis* **2021**, *42* (23), 2445–2464. https://doi.org/10.1002/elps.202100123.
(8) Lapizco-Encinas, B. H. The Latest Advances on Nonlinear Insulator-Based Electrokinetic Microsystems under Direct Current and Low-Frequency Alternating Current Fields: A Review. *Analytical and Bioanalytical Chemistry*. Springer October 19, 2022, pp 885–905. https://doi.org/10.1007/s00216-021-03687-9.

(9) Lapizco-Encinas, B. H. Microscale Nonlinear Electrokinetics for the Analysis of Cellular Materials in Clinical Applications: A Review. *Microchim. Acta* **2021**, *188* (3), 104. https://doi.org/10.1007/s00604-021-04748-7.
(10) Lentz, C. J.; Hidalgo-Caballero, S.; Lapizco-Encinas, B. H. Low Frequency Cyclical Potentials for Fine Tuning Insulator-Based Dielectrophoretic Separations. *Biomicrofluidics* **2019**, *13* (4), 044114. https://doi.org/10.1063/1.5115153.
(11) Hill, N.; Lapizco-Encinas, B. H. Continuous Flow Separation of Particles with Insulator-Based Dielectrophoresis Chromatography. *Anal. Bioanal. Chem.* **2020**, *412* (16), 3891–3902. https://doi.org/10.1007/s00216-019-02308-w.
(12) Jellema, L. C.; Mey, T.; Koster, S.; Verpoorte, E. Charge-Based Particle Separation in Microfluidic Devices Using Combined Hydrodynamic and Electrokinetic Effects. *Lab Chip* **2009**, *9* (13), 1914–1925. https://doi.org/10.1039/b819054b.
(13) Calero, V.; Garcia-Sanchez, P.; Ramos, A.; Morgan, H. Combining DC and AC Electric Fields with Deterministic Lateral Displacement for Micro- And Nano-Particle Separation. *Biomicrofluidics* **2019**, *13* (5), 054110. https://doi.org/10.1063/1.5124475.
(14) Zhu, J.; Xuan, X. Curvature-Induced Dielectrophoresis for Continuous Separation of Particles by Charge in Spiral Microchannels. *Biomicrofluidics* **2011**, *5* (2), 24111. https://doi.org/10.1063/1.3599883.
(15) Patel, S.; Qian, S.; Xuan, X. Reservoir-Based Dielectrophoresis for Microfluidic Particle Separation by Charge. *Electrophoresis* **2013**, *34* (7), 961–968. https://doi.org/10.1002/elps.201200467.
(16) Cardenas-Benitez, B.; Jind, B.; Gallo-Villanueva, R. C.; Martinez-Chapa, S. O.; Lapizco-Encinas, B. H.; Perez-Gonzalez, V. H. Direct Current Electrokinetic Particle Trapping in Insulator-Based Microfluidics: Theory and Experiments. *Anal. Chem.* **2020**, *92* (19), 12871–12879. https://doi.org/10.1021/acs.analchem.0c01303.
(17) Antunez-Vela, S.; Perez-Gonzalez, V. H.; Coll De Peña, A.; Lentz, C. J.; Lapizco-Encinas, B. H. Simultaneous Determination of Linear and Nonlinear Electrophoretic Mobilities of Cells and Microparticles. *Anal. Chem.* **2020**, *92* (22), 14885–14891. https://doi.org/10.1021/acs.analchem.0c03525.
(18) Rouhi Youssefi, M.; Diez, F. J. Ultrafast Electrokinetics. *Electrophoresis* **2016**, *37* (5–6), 692–698. https://doi.org/10.1002/elps.201500392.
(19) Tottori, S.; Misiunas, K.; Keyser, U. F.; Bonthuis, D. J. Nonlinear Electrophoresis of Highly Charged Nonpolarizable Particles. *Phys. Rev. Lett.* **2019**, *123* (1), 14502. https://doi.org/10.1103/PhysRevLett.123.014502.
(20) Hill, N.; Lapizco-Encinas, B. H. On the Use of Correction Factors for the Mathematical Modeling of Insulator Based Dielectrophoretic Devices. *Electrophoresis* **2019**, *40* (18–19), 2541–2552. https://doi.org/10.1002/elps.201900177.
(21) Ruz-Cuen, R.; De Los Santos-Ramírez, J. M.; Cardenas-Benitez, B.; Ramírez-Murillo, C. J.; Miller, A.; Hakim, K.; Lapizco-Encinas, B. H.; Perez-Gonzalez, V. H. Amplification Factor in DC Insulator-Based Electrokinetic Devices: A Theoretical, Numerical, and Experimental Approach to Operation Voltage Reduction for Particle Trapping. *Lab Chip* **2021**, *21* (23), 4596–4607. https://doi.org/10.1039/d1lc00614b.
(22) Coll De Peña, A.; Miller, A.; Lentz, C. J.; Hill, N.; Parthasarathy, A.; Hudson, A. O.; Lapizco-Encinas, B. H. Creation of an Electrokinetic Characterization Library for the Detection and Identification of Biological Cells. *Anal. Bioanal. Chem.* **2020**, *412* (16), 3935–3945. https://doi.org/10.1007/s00216-020-02621-9.
(23) Malekanfard, A.; Beladi-Behbahani, S.; Tzeng, T.-R.; Zhao, H.; Xuan, X. AC Insulator-Based Dielectrophoretic Focusing of Particles and Cells in an "Infinite" Microchannel. *Anal. Chem.* **2021**, *93* (14), 5947–5953. https://doi.org/10.1021/acs.analchem.1c00697.
(24) Saucedo-Espinosa, M. A.; Lapizco-Encinas, B. H. Experimental and Theoretical Study of Dielectrophoretic Particle Trapping in Arrays of Insulating Structures: Effect of Particle Size and Shape. *Electrophoresis* **2015**, *36* (9–10), 1086–1097. https://doi.org/10.1002/elps.201400408.
(25) Saucedo-Espinosa, M. A.; Lapizco-Encinas, B. H. Refinement of Current Monitoring Methodology for Electroosmotic Flow Assessment under Low Ionic Strength Conditions. *Biomicrofluidics* **2016**, *10* (3), 033104. https://doi.org/10.1063/1.4953183.
(26) Breadmore, M. C. Electrokinetic and Hydrodynamic Injection: Making the Right Choice for Capillary Electrophoresis. *Bioanalysis*. Future Science Ltd 2009, pp 889–894. https://doi.org/10.4155/bio.09.73.
(27) Saucedo-Espinosa, M. A.; Lapizco-Encinas, B. H. Exploiting Particle Mutual Interactions To Enable Challenging Dielectrophoretic Processes. *Anal. Chem.* **2017**, *89* (16), 8459–8467. https://doi.org/10.1021/acs.analchem.7b02008.
(28) Saucedo-Espinosa, M. A.; Lalonde, A.; Gencoglu, A.; Romero-Creel, M. F.; Dolas, J. R.; Lapizco-Encinas, B. H. Dielectrophoretic Manipulation of Particle Mixtures Employing Asymmetric Insulating Posts. *Electrophoresis* **2016**, *37* (2), 282–290. https://doi.org/https://analyticalsciencejournals.onlinelibrary.wiley.com/doi/abs/10.1002/elps.201500195.
(29) Leclercq, L.; Morvan, M.; Koch, J.; Neusüß, C.; Cottet, H. Modulation of the Electroosmotic Mobility Using Polyelectrolyte Multilayer Coatings for Protein Analysis by Capillary Electrophoresis. *Anal. Chim. Acta* **2019**, *1057*, 152–161. https://doi.org/https://doi.org/10.1016/j.aca.2019.01.008.

Table of Contents Only